RESEARCH ARTICLE | *Sensory Processing*

Transcranial alternating current stimulation attenuates BOLD adaptation and increases functional connectivity

Kohitij Kar, Takuya Ito, Michael W. Cole, and 🔵 **Bart Krekelberg**
Center for Molecular and Behavioral Neuroscience, Rutgers University-Newark, Newark, New Jersey

Kar K, Ito T, Cole MW, Krekelberg B. Transcranial alternating current stimulation attenuates BOLD adaptation and increases functional connectivity. *J Neurophysiol* 123: 428–438, 2020. First published December 11, 2019; doi:10.1152/jn.00376.2019.—Transcranial alternating current stimulation (tACS) is used as a noninvasive tool for cognitive enhancement and clinical applications. The physiological effects of tACS, however, are complex and poorly understood. Most studies of tACS focus on its ability to entrain brain oscillations, but our behavioral results in humans and extracellular recordings in nonhuman primates support the view that tACS at 10 Hz also affects brain function by reducing sensory adaptation. Our primary goal in the present study is to test this hypothesis using blood oxygen level-dependent (BOLD) imaging in human subjects. Using concurrent functional magnetic resonance imaging (fMRI) and tACS, and a motion adaptation paradigm developed to quantify BOLD adaptation, we show that tACS significantly attenuates adaptation in the human motion area (hMT+). In addition, an exploratory analysis shows that tACS increases functional connectivity of the stimulated hMT+ with the rest of the brain and the dorsal attention network in particular. Based on field estimates from individualized head models, we relate these changes to the strength of tACS-induced electric fields. Specifically, we report that functional connectivity (between hMT+ and any other region of interest) increases in proportion to the field strength in the region of interest. These findings add support for the claim that weak 10-Hz currents applied to the scalp modulate both local and global measures of brain activity.

NEW & NOTEWORTHY Concurrent transcranial alternating current stimulation (tACS) and functional MRI show that tACS affects the human brain by attenuating adaptation and increasing functional connectivity in a dose-dependent manner. This work is important for our basic understanding of what tACS does, but also for therapeutic applications, which need insight into the full range of ways in which tACS affects the brain.

BOLD, fMRI; functional connectivity; motion adaptation; transcranial alternating current stimulation

INTRODUCTION

Weak alternating currents applied to the scalp modulate behavior (Antal et al. 2008; Helfrich et al. 2014a; Kar and Krekelberg 2014), but the mechanistic route from currents on the scalp via changes in neural activity to behavioral change is far from understood (Liu et al. 2018). Our goal is to develop insight into the neural changes caused by transcranial alternating currents and, ultimately, use this insight to improve the transcranial stimulation technique.

Current experimental evidence supports the view that alternating currents can entrain single neurons or networks of neurons and modulate ongoing oscillations (Ali et al. 2013; Francis et al. 2003; Fröhlich and McCormick 2010; Krause et al. 2019; Ozen et al. 2010; Zaehle et al. 2010). Given sufficiently long stimulation periods, this entrainment can outlast stimulation (Helfrich et al. 2014b; Kar 2015). At the cellular level, entrainment is thought to result from the subthreshold modulation of the membrane potential by the weak intracranial electric field generated by the applied currents (Herrmann et al. 2013). Previous studies combining blood oxygen level-dependent (BOLD) imaging with transcranial alternating current stimulation (tACS) have focused primarily on this mode of action. Yet, the experimental results have been equivocal, with both BOLD signal increases and decreases reported (Alekseichuk et al. 2016; Cabral-Calderin et al. 2016a; Vosskuhl et al. 2016).

Recently, we used extracellular recordings in macaque middle temporal cortex (MT) to show that tACS at 10 Hz attenuated sensory adaptation (Kar et al. 2017). This required only a brief period of stimulation (3 s) and primarily affected neurons that were actively responding to the sensory input. These two properties potentially enhance the temporal and functional specificity of tACS. Our specific goal in the current study was to show that attenuation of adaptation also occurs in the human brain. We pursued this question by quantifying BOLD signal changes evoked by sensory (visual motion) adaptation in the presence or absence of tACS.

Previous functional magnetic resonance imaging (fMRI) studies have identified an area in the human brain (hMT+) that, just as MT in the macaque, is highly selective for visual motion (Tootell et al. 1995). The BOLD response of this area is typically reduced after prolonged exposure to moving patterns (Huk et al. 2001), and this so-called BOLD adaptation is generally accepted as a reflection of neuronal adaptation (Krekelberg et al. 2006a), similar to what is observed in single neurons in the macaque (Kar and Krekelberg 2016; Krekelberg et al. 2006b). As such, this brain area is highly suitable to help determine whether findings based on invasive recordings in the animal brain translate to the human brain; it is the primary focus of our study.

Address for reprint requests and other correspondence: B. Krekelberg, Center for Molecular and Behavioral Neuroscience, Rutgers University-Newark, 197 University Ave., Newark, NJ 07102 (e-mail: bart@vision.rutgers.edu).

Beyond providing support for our hypothesis that tACS reduces sensory adaptation, we also used this whole brain data set to investigate whether tACS affects functional connectivity. We found that, indeed, tACS increases functional connectivity and that across regions of interest (ROI), these increases are correlated with the local tACS-induced field strength estimated from individualized head models. Although exploratory, these analyses add to the growing evidence that weak currents applied to the scalp can affect brain activity in complex ways. Overall, we argue that although tACS clearly does modulate the brain in terms of adaptation as well as functional connectivity, much more work is needed to understand its often complex properties and to develop a noninvasive technique that can reliably target specific cortical areas, identified networks, or brain functions.

MATERIALS AND METHODS

Subjects

Ten subjects (5 women) participated in the study. Subjects gave written informed consent, and all had normal or corrected-to-normal vision. The study adhered to the principles expressed in the Declaration of Helsinki and was approved by the Institutional Review Board of Rutgers University.

tACS

We combined transcranial current stimulation with MRI acquisition, which has previously been shown to be safe and results in minimal artifacts and loss of signal to noise (Antal et al. 2014; Williams et al. 2017). The stimulus generator was in the control room and was connected to the electrodes on the subject's head via wall-mounted radiofrequency (RF) filters and MR-compatible, shielded cables (MRIRFIF and custom CBL200; Biopac). The electrode leads were equipped with a 5.6-kΩ resistor to limit RF heating of the head.

In addition, we placed each lead in a neoprene covering to avoid overlapping wires and wire loops, and thus limit current induction. The leads were passed out through the side of the head coil and then led along the bore toward the back of the scanner.

We applied tACS using an STG4002 stimulus generator (Multi Channel Systems, Reutlingen, Germany). The circular stimulating electrodes (BML Basic Physician's Supply, Inc.) were made of conductive rubber (7.6-cm diameter) and attached to the scalp using Signa electrode gel (Parker Laboratories Inc., Fairfield, NJ). One electrode was placed at the canonical location of left hMT+ (PO7–PO3 in the 10–20 system) and the other on the vertex (Cz). The current amplitude was 0.5 mA (i.e., 1 mA peak to peak); the frequency was 10 Hz. These electrodes and parameters were chosen to match our previous behavioral experiments in humans (Kar and Krekelberg 2014) and electrophysiological recordings in the macaque (Kar et al. 2017).

Apparatus

A Canon REALiS SX80 Mark II LCOS projector (60 Hz) back-projected the stimuli onto a screen located at the end of the MRI bore. Subjects viewed the stimuli via a mirror attached to the head coil. The combined distance of the screen to the mirror and the mirror to the subjects' eyes was 103 cm. The display measured 22° (width) by 12° (height) and had a resolution of 1,920 × 1,080 pixels. Stimulus presentation and the triggering of stimulation were under the control of in-house, OpenGL-based software.

Motion Adaptation Paradigm

We adopted the paradigm of Huk et al. (2001) to quantify direction-selective motion adaptation in the BOLD signal. Subjects fixated a dot at the center of the screen while viewing two moving gratings on either side of the dot (5° × 5° centered on ±7°; Fig. 1A). Trials were classified into two conditions. As shown in Fig. 1B, top, in the "adapted test-direction trials" (O), the adapter (A_o; gratings moving outward for 4 s) was followed by a test stimulus that also moved
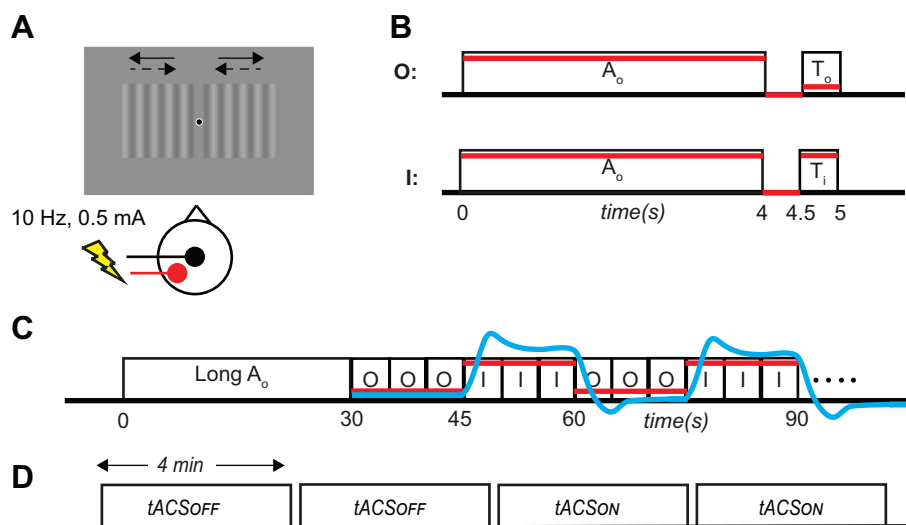

Fig. 1. Experimental paradigm. *A*: one stimulation electrode was placed on the vertex (Cz; black) and one on PO7–PO3 (red). Subjects were instructed to fixate on the central black dot on the screen throughout the experiment. The visual stimulus was a sinusoidal grating that could drift outward (solid arrows; A_o and T_o) or inward (dashed arrows; T_i). *B*: structure of individual trials. In outward (O) trials, the outward moving adapter (A_o) was followed by an outward-moving test stimulus (T_o). In inward (I) trials, the same outward-moving adapter was followed by an inward moving test stimulus (T_i). Red lines show a prediction of the neural activity in human motion area (hMT+) in each of these trials; adaptation to outward motion should reduce the response to the outward test stimulus (T_o) but not to the inward test stimulus (T_i). *C*: structure of an experimental run. Each run started with a 30-s presentation of A_o followed by alternating blocks of 3 O and 3 I trials. Red lines show the prediction of neural activity at the block level. In a voxel that adapts, neural activity should be lower in 3 successive O trials than in 3 successive I trials. Blue line shows the shape of the predicted hemodynamic signal (based on a canonical hemodynamic response function; see MATERIALS AND METHODS). Note that the vertical axes of *B* and *C* are not to scale. *D*: structure of a session. Each subject participated in 2 runs without transcranial alternating current stimulation (tACS_OFF) followed by 2 runs with stimulation (tACS_ON).

outward (T_o: 0.5 s). In "nonadapted test-direction trials" (I), the same adapter, A_o, was followed by a test stimulus moving inward for 0.5 s (T_i). Figure 1*C* shows that each run started with a 30-s presentation of the adapter (A_o) followed by repeated blocks of three adapted test direction (outward) trials (O in Fig. 1*C*) and three nonadapted test-direction trials (I in Fig. 1*C*). The main advantage of this somewhat complex arrangement of conditions is that it induces a strong level of adaptation (by the long adapter) that is maintained at a steady level (by the repeated presentation of the top-up adapter A_o), interspersed with brief measurements of the state of adaptation (by the response to the test stimuli T_o/T_i). Moreover, using three successive trials with the same test direction creates blocks of 15 s, which is well suited for the block-based fMRI analysis (below). Each block was repeated seven times per run. Each subject participated in four experimental runs in the same session (Fig. 1*D*), two without tACS (tACS$_{OFF}$) followed by two with tACS (tACS$_{ON}$). In the tACS$_{ON}$ conditions, the current was applied whenever the adapter stimulus [either the long adapter (long A_o) or the top-up adapter (A_o)] was on the screen (i.e., during the induction of adaptation).

fMRI Data Acquisition

We conducted all imaging at the Rutgers University Brain Imaging Center using a 3T MRI (Tim Trio, Siemens) scanner and a 32-channel head coil with ample padding around the head to minimize head movement. We used a T1-weighted magnetization-prepared rapid gradient-echo (MPRAGE) sequence to collect anatomical images (1-mm³ resolution) from each subject. For functional scans, we used a T2*-weighted echo planar imaging (EPI) sequence (repetition time = 2 s, echo time = 25 ms, flip angle = 90°, matrix = 64 × 64). The 35 slices (in-plane resolution = 3 × 3 mm, slice thickness = 3 mm) covered the entire brain and were oriented approximately parallel to the line connecting the anterior to the posterior commissure.

Data Analysis

Adaptation analysis. DATA PREPROCESSING. We analyzed the fMRI data with BrainVoyager (version 2.6; Brain Innovation, Maastricht, The Netherlands) and MATLAB (MathWorks). After discarding the first nine volumes of each functional scan, we performed linear trend removal, slice scan time adjustment, three-dimensional (3-D) motion correction with alignment to the first volume within an MRI session, and temporal filtering using a high-pass filter with a 0.0078-Hz cutoff. The functional images were superimposed on the high-resolution anatomical images and incorporated into the 3-D data sets through trilinear interpolation. The complete data set was transformed into Talairach space. We defined area hMT+ by a sphere (10-mm radius) around its canonical Talairach coordinates: (40, −60, 0) for the right hemisphere and (−40, −60, 0) for the left hemisphere.

BOLD ADAPTATION. Based on the known adaptation properties of MT neurons in the macaque (Kar and Krekelberg 2016; Krekelberg et al. 2006b; Patterson et al. 2014) and previous studies in humans (Huk et al. 2001; Tootell et al. 1995), we predicted that for our choice of stimuli, adaptation would primarily reduce the neural response in the adapted-direction trials compared with the opposite-direction trials. In Fig. 1*B*, this means that the neural responses to each of the T_o stimuli is expected to be smaller than the neural response to T_i (red lines in Fig. 1*B*) At the block level, we model this expectation as a neural response that is higher in the nonadapted direction trials (I) than in the adapted direction trials (O) (red lines in Fig. 1*C*). To account for the dynamics of the hemodynamic response, we convolved this block-level prediction with a canonical two-gamma hemodynamic response function (HRF; onset = 0 s, response to undershoot ratio = 6, time to response peak = 5 s, time to undershoot peak = 15 s, response and undershoot dispersion = 1). The blue curve in Fig. 1*C* illustrates the shape of the resulting "adaptation predictor."

We quantified the strength of direction-selective adaptation (α^{DS}) for each voxel as the Pearson correlation between the adaptation predictor and the BOLD time course of the voxel. Voxels with a positive α^{DS} value show the expected effect of adaptation (Huk et al. 2001): a neural response that is lower when the test moves in the same direction as the adapter than when the test moves in the opposite direction. To arrive at a single adaptation measure for each hMT+ (i.e., per subject, per hemisphere), we averaged the α^{DS} over all voxels within the anatomically defined ROIs (see above). For all statistical analyses, we used the Fisher z transform to create a statistic with an asymptotic normal distribution. From this, we estimated the confidence intervals at the single-subject level (see Figs. 2 and 5). Also, at the group level, we used the Fisher z-transformed mean α^{DS} as the dependent variable in a mixed-effects model with stimulation condition (tACS$_{ON}$/tACS$_{OFF}$) and hemisphere (left/right) as fixed effects and an intercept per subject as a random effect. Unless otherwise noted, statistical inferences were derived from this model using maximum likelihood estimation and a significance threshold of 0.05. For each statistical inference, we report the corresponding t statistic and its degrees of freedom.

Functional connectivity analysis. DATA PREPROCESSING. All connectivity preprocessing and analyses were performed using MATLAB and AFNI (version 2011-12-21; Cox 1996). The first nine volumes of each scan were discarded to reduce the influence of transients on data analyses. EPI images were slice-time corrected, aligned to the subject's skull-stripped MPRAGE in native space, motion corrected, and transformed to Talairach space. A linear regression was subsequently performed to remove nuisance parameters from the time series. This included the six motion parameters, ventricle and white matter time series along with their derivative time series. In addition, to remove any potential spatial co-activation confounds with functional connectivity (FC) analyses, we also regressed out event-averaged BOLD signals related to stimulus presentation (adapter on/off, test on/off, and tACS on/off), all convolved with the same canonical HRF as in the above-described adaptation analysis (Cole et al. 2019). The residual time series was then spatially smoothed within a one-voxel dilated gray matter mask at 6-mm full-width half-maximum.

ROI-BASED FUNCTIONAL CONNECTIVITY ANALYSIS. Because our paradigm was specifically targeted to drive visual responses (and adaptation) in hMT+, we chose these areas as the primary seeds for our FC analyses and the 264 predefined functional regions of the Power et al. (2011) atlas as the target regions. The spherical size of the ROIs in the Power atlas have a 5-mm radius. To match this scale, we defined left and right hMT+ by a 5-mm radius sphere around their canonical coordinates (as opposed to the 10-mm radius used in the adaptation analysis described above). We removed regions 257 and 262 from the Power atlas for our analyses, because they either overlapped or were adjacent to the left and right hMT+. For each ROI, we first split up the time series according to stimulation condition (tACS$_{OFF}$ and tACS$_{ON}$) and direction of motion (nonadapted direction and adapted direction). We then computed the Pearson correlation between each of the hMT+ and all other regions to obtain FC measures for each of the conditions, resulting in four connectivity vectors for each hMT+. We removed negative FC connections and self-connections, because they likely reflect spurious connections that add noise to the underlying network topology (Rubinov and Sporns 2010).

For each target area, we entered the Fisher z-transformed correlations (i.e., the functional connectivity of left and right hMT+ with the target area) as the dependent variable in a four-way mixed-effects model with direction, stimulation, and hemisphere as fixed effects and an intercept per subject as a random effect. In this model, a significant two-way interaction between stimulation and hemisphere indicates an effect of stimulation that can be attributed to the difference in electric field strength induced in left and right hMT+ (see RESULTS). However, if this effect occurs in the presence of a significant three-way inter-

action between stimulation, hemisphere, and direction, then this FC change could potentially be accounted for by a change in adapted state (i.e., it could be a follow-on effect of the attenuation of adaptation). Therefore, we searched specifically for pairs with significant two-way interactions between stimulation and hemisphere that occurred in the absence of the above three-way interaction. Only those pairs are reported below as showing a significant effect of tACS on FC. All P values were corrected for multiple comparisons with the false discovery rate (FDR) procedure.

Field strength. We used the Realistic vOlumetric-Approach to Simulate Transcranial Electric Stimulation (ROAST; version 4.11) pipeline (Huang et al. 2019) to model electric field strengths based on the subjects' individual structural T1-weighted MRI and on the Montreal Neurological Institute (MNI) template brain (MNINLin6Asym). All ROAST simulations used tissue conductivity parameters from the literature (Huang et al. 2017) (white matter: 0.126 S/m, gray matter: 0.276 S/m, cerebrospinal fluid: 1.65 S/m, bone: 0.01 S/m, and skin: 0.456 S/m). We used fMRIPrep (version 1.4.1rc1; Esteban et al. 2019) to determine the spatial transforms necessary to normalize each subject's T1 to the MNI template (at 2-mm resolution) and then applied that same transform to the electric field magnitude computed by ROAST. From these model results in the MNI space, we extracted the field magnitude in the voxels corresponding to hMT+ and the ROIs of the Power atlas. The field magnitude of an ROI was defined as the median field magnitude across its voxels.

If tACS-induced fields modulate adaptation or functional connectivity, one would expect that such neural measures are affected most in subjects, ROIs, or networks that receive the strongest electric fields. We used several linear mixed effect models to test this prediction.

In the model describing the link between adaptation and field strength, the dependent variable was α^{DS} for left and right hMT+ (tACS$_{ON}$ blocks only; 20 observations), the fixed effects were the field strengths in left and right hMT+, and as random effects we included an intercept and the field strength grouped by subject.

In the model describing the link between global brain connectivity (GBC) changes and field strength, the dependent variable was the difference in GBC in the tACS$_{ON}$ and tACS$_{OFF}$ blocks, for each ROI (262 from the Power atlas plus left and right hMT+) and each subject (ΔGBC: 2,640 observations). The fixed effect was the field strength in each ROI, and we included an intercept and the field strength as a random effect for subjects. We also constructed a model that compared changes in GBC between mirrored ROIs in the left and right hemisphere and related it to the ratio of the field strengths in the mirrored ROIs. This model has the advantages that intrinsic differences in GBC across ROIs are subtracted (to the extent that left and right hemispheres are similar) and that the potential confound of time is removed. To identify these mirror ROIs, we extracted the MNI coordinates of the ROIs in the left hemisphere (x, y, z, with $x < 0$) and then searched for ROIs whose center was within 5 mm from ($-x$, y, z). In the Power atlas, 31 ROIs met this criterion. For each mirror pair, we then calculated ΔGBC$_{L-R}$ = ΔGBC (left-hemisphere ROI) − ΔGBC(mirror ROI). The dependent variable in the model was ΔGBC$_{L-R}$ (310 observations), the field ratio was modeled as a fixed effect, and we included an intercept and the field ratio as a random effect per subject.

We followed an analogous approach to study FC differences. In the model describing the main effect of stimulation at the ROI level, the dependent variable was the tACS-induced difference in FC between hMT+ and the target ROIs of the Power atlas. For each ROI it is defined as the difference between FC in the tACS$_{ON}$ and tACS$_{OFF}$ blocks: ΔFC = FC(tACS$_{ON}$) − FC(tACS$_{OFF}$). With 10 subjects, 262 target ROIs (264 in the atlas minus the 2 that overlap with hMT+; see above), and 2 hMT+ seed regions, this model has 5,240 observations. The model included field strength in each target ROI, the hMT+ hemisphere, and their interaction as fixed effects, and field strength and an intercept as a random effect across subjects.

Because tACS$_{ON}$ blocks always followed tACS$_{OFF}$ blocks, the analysis of ΔFC is potentially confounded with the passage of time. To remove this confound, we also quantified how the difference in ΔFC between left hMT+ and right hMT+ was affected by the field strength in the target ROI. In this linear mixed-effects model, ΔFC$_{L-R}$ is the dependent variable (2,620 observations), the field strength in each target ROI was modeled as a fixed effect, and we included field strength and an intercept as a random effect per subject.

For an analogous analysis at the network level, we needed to define a single measure of field strength and ΔFC for each of the 13 networks in the Power atlas. These networks are distributed spatially and often contained a wide range of field strengths. Because a strong field in only a part of the network could still be an effective modulator of that network, we defined the field strength of each network as the 90th percentile of the field magnitudes of its constituent voxels. Similarly, for the purpose of this analysis, the change in FC of a network (ΔFC^N) was defined as the 90th percentile of the changes in FC of its constituent ROIs. We note, however, that qualitatively similar relationships between field strength and ΔFC^N were found for other definitions (e.g., taking the 50th percentile for field strength or ΔFC^N changes across a network).

At the network level, the linear model describing the main effect of stimulation used ΔFC^N as its dependent variable (13 networks, 2 hMT+ seed regions = 260 observations), network field strength, MT hemifield, and their interaction as fixed effects, and an intercept and network field strength grouped by subject as random effects. As before, to remove the potential confound of time, we also constructed a model comparing changes in FC to left and right hMT+: ΔFC$^N_{L-R}$ = ΔFC^N(left hMT+) − ΔFC^N(right hMT+) (130 observations), with field in the target ROI as a fixed effect, and an intercept and field strength as a random across-subjects effect.

RESULTS

Using concurrent fMRI and tACS in healthy human volunteers, we investigated whether tACS ($\pm$0.5 mA, 10 Hz) changed neural activity while the subjects passively viewed moving patterns. We report three complementary findings. First, we found that tACS reduced sensory adaptation of the human motion area. Second, we found that tACS increased functional connectivity. Third, we found that both the reduction of adaptation and the increased FC depended strongly on the magnitude of the tACS-induced field. This was the case across subjects (less adaptation in subjects with larger tACS-induced intracranial fields) and across regions of interest (more increases in FC in regions with larger fields).

tACS Reduces Adaptation in hMT+

A long line of research has shown that exposure to a moving pattern (i.e., motion adaptation) evokes direction-specific aftereffects that can be quantified using behavioral, imaging, and electrophysiological methods (Anstis et al. 1998; Kohn 2007). We used the method of Huk et al. (2001) to measure the strength of direction-selective adaptation in hMT+. Subjects were instructed to fixate a central fixation point while the visual stimulus (a set of sinusoidal gratings) drifted outward or inward (Fig. 1A). Each trial started with a 4-s presentation of an outward-moving adapting grating (adapter: A$_o$), followed by a brief blank (0.5-s gray screen) and then a 0.5-s test stimulus. In adapted test-direction trials, the test stimulus moved in the same outward direction as the adapter (T$_o$; Fig. 1B, *top*). In nonadapted test-direction trials, the test stimulus moved in the inward direction (T$_i$; Fig. 1B, *bottom*). A block consisted of three successive trials of the same type (O, outward/
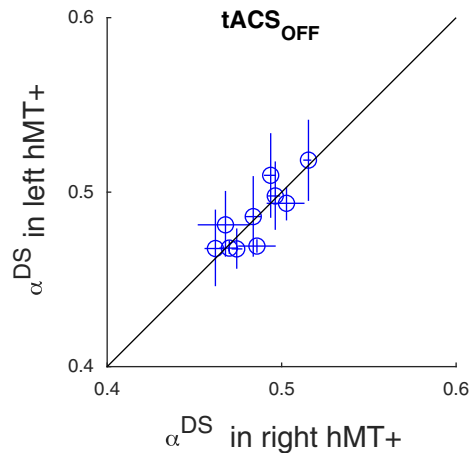
Fig. 2. Blood oxygen level-dependent (BOLD) adaptation in the absence of transcranial alternating current stimulation (tACS). Each data point corresponds to a single subject and compares the mean direction-selective adaptation (α^{DS}) in the left (y-axis) and right (x-axis) human motion area (hMT+). Error bars represent 95% confidence intervals. Replicating the findings of Huk et al. (2001), hMT+ showed adaptation of the BOLD signal due to sensory adaptation ($\alpha^{DS} > 0$). This effect did not differ between the hemispheres.

adapted test direction or I, inward/nonadapted test direction), and each run contained seven alternating blocks of the O/I type (Fig. 1C).

Adaptation effects increase with the duration of exposure over tens of seconds, but to avoid overly long experiments, researchers typically use a so-called top-up paradigm. In this paradigm, a series of trials with brief presentations of the same adapter (here A_o) is preceded by a long (several tens of seconds) exposure to that pattern. This sequence creates aftereffects that are similar to experiments in which the long exposure adapter is used in every trial but allows the collection of many more trials in the same amount of time. Not surprisingly, the top-up paradigm is commonly used in fMRI studies (Engel 2005; Fang et al. 2005; Larsson et al. 2005). In this study we used an initial exposure of 30 s (long A_o; Fig. 1C).

In an fMRI voxel, we expect there to be an approximately equal number of neurons responding to inward and outward motion. After adaptation to outward motion, however, the response to outward motion should be less than that to inward motion, because the outward preferring neurons (but not the inward preferring neurons) have a reduced firing rate (Kar and Krekelberg 2016; Krekelberg et al. 2006a). The red curves show a cartoon neural prediction at the trial level in Fig. 1B and at the block level in Fig. 1C. To arrive at a prediction for the BOLD signal, we convolved this block-level neural prediction with the canonical hemodynamic response function (see MATERIALS AND METHODS). The correlation (α^{DS}; see MATERIALS AND METHODS) between this predictor (blue curve in Fig. 1C) and the observed BOLD response quantifies not the activity, but the adaptation per voxel (Huk et al. 2001). Our primary goal in this study was to determine whether tACS affects α^{DS}.

We placed one stimulation electrode approximately over left hMT+ (between PO3 and PO7 in the 10–20 system) and the other over the vertex (Cz) and applied a sinusoidal current with a frequency of 10 Hz and amplitude of 0.5 mA (Fig. 1A). This matched our previous study documenting the behavioral consequences of applying tACS during motion adaptation (Kar and Krekelberg 2014). In each session, a subject first com-

pleted two runs without tACS and then two runs with tACS (Fig. 1D)

First, we confirmed that our experiment replicated the findings of (Huk et al. 2001). In the absence of stimulation (i.e., analyzing only the tACS$_{OFF}$ blocks), the bilateral adaptation stimulus led to significant BOLD adaptation in both the left hMT+ [$\alpha^{DS} = 0.49$ (SD 0.019)] and the right hMT+ [$\alpha^{DS} = 0.49$ (SD 0.017)]. Adaptation was significantly larger than zero [$t(18) = 75$, $P = $ 6e-24] and did not differ between the hemispheres [$t(18) = 0.1$, $P = 0.9$]. Figure 2 shows a direct comparison of α^{DS} across hemispheres in the tACS$_{OFF}$ blocks.

Second, we investigated the main effect of stimulation. We predicted that adaptation should be smaller in the tACS$_{ON}$ compared with the tACS$_{OFF}$ conditions. Figure 3 shows histograms of the strength of adaptation for the tACS$_{OFF}$ (blue) and tACS$_{ON}$ (red) conditions (pooled over left and right hMT+). The mean adaptation in the tACS$_{ON}$ condition was much smaller than in the tACS$_{OFF}$ blocks [$t(36) = -26.9$, $P = $ 2e-25].

In our experimental design, the two tACS$_{OFF}$ blocks always preceded the two tACS$_{ON}$ blocks (Fig. 1D). Although this design is useful to prevent aftereffects of stimulation from contaminating later BOLD signals (Cabral-Calderin et al. 2016a), it creates a confound between a main effect of stimulation (i.e., the comparison of tACS$_{OFF}$ and tACS$_{ON}$ blocks) and the mere passage of time. It seems unlikely that this confound can fully account for the large differences in adaptation (Fig. 3) between the blocks. First, our preprocessing procedures (see MATERIALS AND METHODS) removed slow (scanner) signal drift, and even more to the point, our variable of interest (α^{DS}) is a correlation measure that is insensitive to overall signal changes that are uncorrelated with the specific predictions based on the neurophysiology of adaptation (Fig. 1C). To explain the reported main effect of stimulation (Fig. 3), passage of time would have to result in reduced adaptation. We
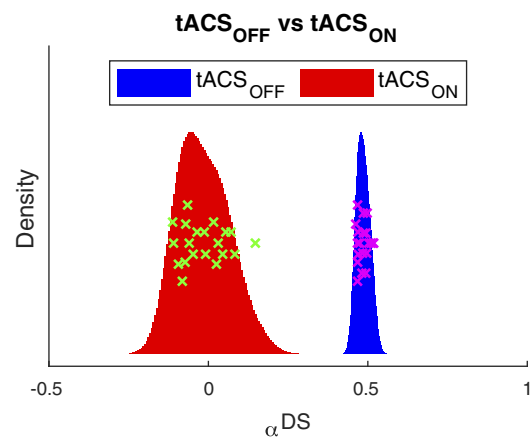

Fig. 3. Transcranial alternating current stimulation (tACS) reduces blood oxygen level-dependent adaptation in human motion area (hMT+). Histograms show the distribution of the strength of adaptation (α^{DS}) in left and right hMT+ separately for the blocks without (tACS$_{OFF}$; blue) and with (tACS$_{ON}$; red) stimulation. Data points (one cross for each left and right hMT+ in each subject) illustrate the variability separately for tACS$_{OFF}$ (magenta) and tACS$_{ON}$ (green). The vertical position of these points carries no meaning; it serves only to separate the points. The histograms were estimated using a normal kernel density estimator; hence, the y-position represents the relative density/probability of the corresponding adaptation value on the x-axis. Adaptation was much reduced in the tACS$_{ON}$ blocks compared with the tACS$_{OFF}$ blocks.
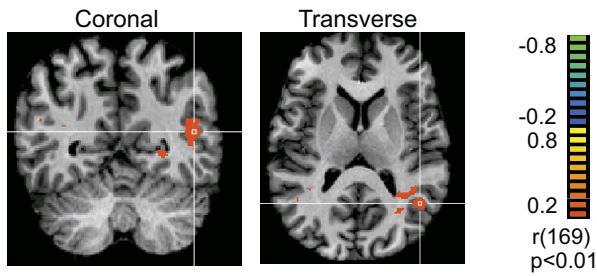
Coronal   Transverse

Fig. 4. Transcranial alternating current stimulation (tACS) reduces blood oxygen level-dependent (BOLD) adaptation more in left human motion area (hMT+) than in right hMT+. In these data from an individual subject, color maps show the amount of BOLD adaptation (α^{DS}) per voxel (see MATERIALS AND METHODS). Images are in radiological convention. White crosshairs in the coronal and sagittal slices are at Talairach (x, y, z) coordinates $(40, -72, -7)$. Adaptation in hMT+ of the left hemisphere, which received a twofold stronger electric field, was much less pronounced than adaptation in the right hemisphere.

Fig. 5. Transcranial alternating current stimulation (tACS$_{ON}$) reduces blood oxygen level-dependent (BOLD) adaptation more in left human motion area (hMT+) than in right hMT+. Each data point corresponds to a single subject and compares the mean adaptation (α^{DS}) in the left (y-axis) and right (x-axis) hMT+. Error bars represent 95% confidence intervals. Adaptation was weaker in left than right hMT+, supporting the claim that the stronger tACS field in left hMT+ led to a stronger reduction of adaptation.

are not aware of any evidence supporting this. In fact, motion adaptation can be induced reliably and repeatedly across extended periods of time in humans and monkeys (Kar and Krekelberg 2016; Krekelberg et al. 2006b; Patterson et al. 2014) and does not seem to abate over the typical time course of an experiment. We also investigated this directly in our data set. If adaptation decreased over time (i.e., even without the presence of current stimulation), one would predict that α^{DS} in the first tACS$_{OFF}$ run would be larger than α^{DS} in the second tACS$_{OFF}$ run. Contrary to this, we found a nominal increase in α^{DS} that was not statistically significant [first block: 0.48 (SD 0.02), second block: 0.50 (SD 0.04), $t(38) = 1.38$, $P = 0.08$]. Hence, we conclude that it is unlikely that time alone caused the reduction in adaptation that we ascribe to tACS.

Third, we investigated the interaction between field strength (i.e., hemisphere) and adaptation. As discussed in detail below, left hMT+ received a field that was approximately twice the magnitude of that in right hMT+. Therefore, we predicted that adaptation in left hMT+ should be smaller (reduced more) than in right hMT+. Figure 4 shows the voxelwise strength of adaptation (α^{DS}) from one example subject in the tACS$_{ON}$ trials. The red clusters show the voxels that adapted significantly (thresholded at $\alpha^{DS} = \pm 0.2$; $P = 0.01$). Clearly, this subject had fewer significantly adapted voxels in the left than the right hemisphere and the subject's mean α^{DS} in left hMT+ was smaller than in right hMT+. This hemisphere-specific stimulation effect was consistent across subjects. Figure 5 visualizes this by plotting α^{DS} in left hMT+ as a function of α^{DS} in right hMT+. We quantified its statistical significance first with a direct comparison, showing that during the tACS$_{ON}$ blocks, adaptation in left hMT+ was smaller than in right hMT+ [$t(18) = 3.96$, $P = 0.0009$]. For completeness, we also compared the difference between left and right hMT+ in the tACS$_{ON}$ blocks with the analogous differences in the tACS$_{OFF}$ blocks; this confirmed that the effect of hemisphere was larger in the tACS$_{ON}$ than in the tACS$_{OFF}$ blocks [paired t test: $t(9) = 3.9$, $P = 0.0035$].

Neurons that respond less typically adapt less (Kar and Krekelberg 2016). Hence, a logical question to ask is whether tACS attenuates adaptation because it decreases overall neural activity (Vosskuhl et al. 2016). This explanation predicts that BOLD signals should be lower during tACS. We evaluated this by comparing the BOLD responses in hMT+ during the long adapter stimulus in the runs when tACS was on with responses
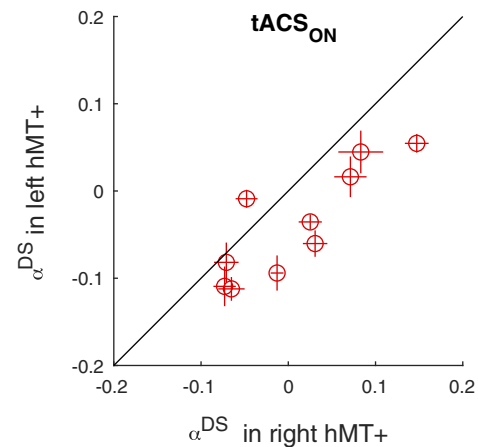
when tACS was off. A two-way repeated-measures ANOVA with hemisphere (stimulated/unstimulated) and tACS (ON/OFF) as factors showed that tACS was associated with a modest increase, and not a decrease, in BOLD response [main effect of tACS: $F(1,9) = 7.8$, $P = 0.02$]. This finding is incompatible with a model in which reduced neuronal firing during tACS results in reduced adaptation (measured after tACS offset). Instead, we speculate that tACS interferes directly with the cellular mechanisms underlying adaptation (see DISCUSSION).

Functional Connectivity

Although the primary goal of our experiment was to test the adaptation hypothesis, the whole brain data allowed us to perform an exploratory analysis of the influence of tACS on functional connectivity (FC). Because our task was designed to drive visual motion areas, we focused on the functional connectivity of hMT+. The seed regions for the FC analysis are shown in Fig. 6A.

Moreover, the goal of this analysis was to determine whether tACS changed FC in a manner that could not be explained on the basis of our primary finding (a change in adaptation). To achieve this, we first regressed out cross-trial means of stimulus-related activity and determined FC of each hMT+ with a set of target areas based on the residual activity only (see
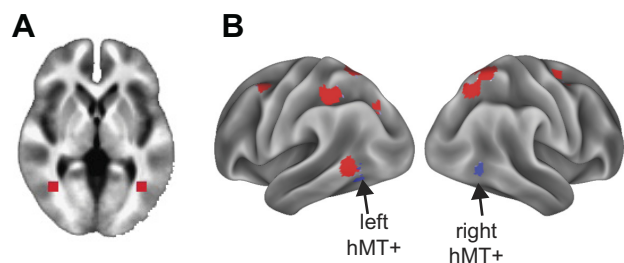

Fig. 6. Functional connectivity analysis. A: bilateral human motion area (hMT+) seeds in volume space at $(40, -60,0)$ and $(-40, -60, 0)$. B: surface visualization of bilateral hMT+ seeds (blue) and dorsal attention network regions (red).

A

left hMT+ (adapt) — left hMT+ (non-adapt)

B

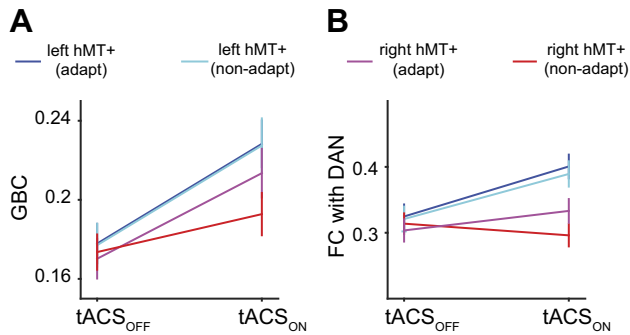right hMT+ (adapt) — right hMT+ (non-adapt)

Fig. 7. Transcranial alternating current stimulation (tACS) increases functional connectivity (FC). *A*: global brain connectivity (GBC) of human motion area (hMT+) increased with tACS, more so in the left hemisphere than in the right hemisphere, and, at least in the left hemisphere, there was no interaction with adaptation. *B*: FC between hMT+ and the dorsal attention network (DAN) increased with tACS, more in the left than in the right hemisphere. Adaptation did not affect this interaction. These analyses show that 10-Hz tACS increases FC and that at least some of this effect (*B*) is distinct from the influence of tACS on adaptation.

MATERIALS AND METHODS). We then specifically searched for tACS-induced FC changes that could be attributed to the different electric fields generated in the two hemispheres (two-way interaction between hemisphere and stimulation; see MATERIALS AND METHODS). Finally, from this set of results, we excluded those pairs in which the effect depended on the direction of test stimulus motion, because that would likely be the result of an effect of adaptation (3-way interaction between hemisphere, stimulation, and direction; see MATERIALS AND METHODS).

At the whole brain level, we computed weighted degree centrality, also known as global brain connectivity (GBC) (Cole et al. 2010, 2012; Ito et al. 2017). This graph theoretic measure represents the average FC of a region to the entire brain (Rubinov and Sporns 2010). We found that tACS significantly increased the GBC of left hMT+ compared with right hMT+ [$F(1,9) = 13.89$; $P = 0.005$]. Figure 7*A* visualizes both the main effect of stimulation (*x*-axis) and the interaction with hemisphere and adaptation (color key).

At the network level, we computed the average FC of left and right hMT+ to the set of predefined functional networks in the Power et al. (2011) atlas. FC with the dorsal attention network (DAN; Fig. 6) increased more for left hMT+ than for right hMT+ [$F(1,9) = 16.20$; $P = 0.04$; FDR corrected].

Figure 7*B* shows the FC measures for the DAN and hMT+. FC changes with any of the other 12 functional networks defined by Power et al. (2011) did not reach significance ($F < 13.90$; $P > 0.05$; FDR corrected).

At the region-to-region level, we computed the FC between hMT+ and the 264 ROIs defined by the Power et al. (2011) atlas. At this level of detail, none of the ROIs showed a significant change in FC with hMT+ after multiple comparison corrections ($F < 21.65$; $P > 0.05$; FDR corrected). In summary, tACS increased FC of hMT+ (ΔFC_{L-R}; see MATERIALS AND METHODS), and this was primarily due to increased connectivity with the dorsal attention network, but the data do not allow us to draw conclusions at a finer spatial scale.

Field Strength

If tACS-induced intracranial fields drive the changes in adaptation and functional connectivity reported above, one would predict that larger intracranial fields should result in larger effects. To investigate this, we constructed finite element current-flow models for each subject using the ROAST pipeline (Huang et al. 2019). From these models we estimated the field strength in left and right hMT+ and the ROIs and networks of the Power atlas (Power et al. 2011). For illustrative purposes, Fig. 8 shows the simulated field magnitudes based on the MNI template (see MATERIALS AND METHODS). These simulations show that our montage did generate relatively strong fields in the targeted left hMT+. However, many other areas also experienced field strengths of similar magnitude. This is an inevitable consequence of using large pad stimulation electrodes (see DISCUSSION). In the following, we analyze the relationship between local field strength and the neural measures presented previously (adaptation, GBC, and FC).

Adaptation. The average electric field magnitude in a sphere centered on left hMT+ was 0.16 V/m (SD 0.02 V/m), whereas right hMT+ received 0.09 V/m (SD 0.01 V/m). The magnitude of these estimated fields depends strongly on the (coarse) estimates of tissue conductivities used in the model and should be taken with a grain of salt. However, the ratio of the field strength in the left vs. right hMT+ is more robust against errors in these assumptions. Therefore, we prefer the quantification in terms of a ratio: tACS induced an electric field in left hMT+ that was 1.8 (SD 0.3) times stronger than in right hMT+ (range: 1.4 to 2.3). In the context of the reduction of
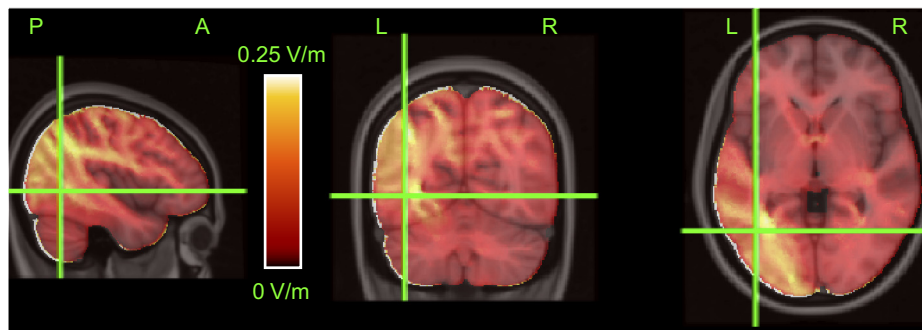

Fig. 8. Intracranial fields. Color represents the magnitude of the estimated fields based on a finite-element current-flow model of the MNI 152 template T1-weighted MRI (see MATERIALS AND METHODS). Color bar shows the mapping between color and field magnitude; the range was clipped at 0.25 V/m to improve visual clarity. Crosshairs identify the nominal center of left human motion area (hMT+), the area of a priori interest. Predominantly hot (yellow) colors near the crosshairs show that field magnitudes in left hMT+ were among the largest, providing post hoc reassurance that our montage did stimulate this area. However, several other regions in parietal and visual cortex received similarly strong stimulation. Labels indicate left (L), right (R), anterior (A), and posterior (P) parts of the brain.

adaptation, these values support our reasoning that one should expect a main effect of stimulation (because both left and right hMT+ were stimulated) and an interaction (left hMT+ was stimulated more than right hMT+). Our results described above confirm both these predictions. Combining field strength estimates with adaptation changes across subjects, we went one step further and determined whether adaptation (α^{DS}) varied with field strength. A linear mixed model, limited to the tACS$_{ON}$ conditions alone, showed that this was indeed the case [$t(18) = -3.75$, $P = 0.001$]. In other words, across subjects, hMT+ ROIs that received stronger fields showed a larger reduction in adaptation.

Global brain connectivity. Next, we investigated whether GBC changes of any ROI were correlated with the tACS-induced field strength of that ROI. First, we calculated the change in GBC for each ROI when applying tACS (i.e., the main effect of stimulation on GBC, ΔGBC) and related this to the field strength in each ROI using a linear mixed model (see MATERIALS AND METHODS). The effect of field strength was highly significant [$t(2368) = 3.52$, $P = 0.0004$], showing that ROIs that received stronger fields increased their GBC more. Because this main effect includes the potentially confounding factor of time, we also performed an interaction analysis using ROI pairs with mirrored locations in the two hemispheres (see MATERIALS AND METHODS). The difference between ΔGBC in mirrored ROIs (ΔGBC$_{L-R}$) depended significantly on the ratio of the field strength in mirrored ROIs [$t(308) = 1.99$, $P = 0.047$]. This supports the claim that even after correction for the potentially confounding influence of time, ROIs with larger field strengths increase their GBC more.

Functional connectivity with hMT+. As discussed above, we focused our FC analysis on hMT+ seeds due to the nature of the task that the subjects performed. We first investigated how local field strength in a target ROI affected its change in FC with the left or right hMT+ seeds. This is the main effect of stimulation: ΔFC (see MATERIALS AND METHODS). Field strength significantly affected ΔFC [$t(5,196) = 2.84$, $P = 0.005$], and there was a significant interaction with hemisphere [$t(5,196) = 2.96$, $P = 0.003$]. This suggests that the effect was mainly driven by changes in left hMT+ (which had the stronger fields). A separate analysis of ΔFC in left and right hMT+ confirmed this; larger fields in an ROI significantly increased ΔFC with left hMT+ [$t(2628) = 2.62$, $P = 0.009$] but not right hMT+ [$t(2,568) = 1.00$, $P = 0.32$]. This is consistent with the interpretation that the fields in right hMT+ were too small to result in increased ΔFC, even with target ROIs that themselves received strong fields.

The preceding FC analysis looked at the main effect of stimulation; to correct for the potential confounding influence of time, we performed an analogous analysis of the interaction effect. Specifically, we defined ΔFC$_{L-R}$ as the difference between ΔFC for left hMT+ and ΔFC for right hMT+ and related this to the field strength in each target ROI. The linear mixed model again showed a significant effect of field strength [$t(2,618) = 2.70$, $P = 0.007$]. This means that tACS increased connectivity between left hMT+ and a target ROI more than connectivity of right hMT+ and the target ROI, and that this difference increased with the field strength in the target ROI.

This relation between field strength and ΔFC$_{L-R}$ changes is visualized in Fig. 9. Across the ROIs, field magnitude (blue) varied between 0 and nearly 0.5 V/m. The red curve represents
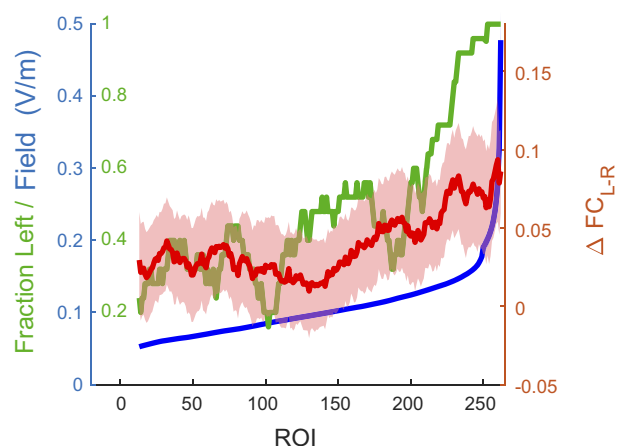

Fig. 9. Transcranial alternating current stimulation (tACS) increases functional connectivity (FC) with human motion area (hMT+) in a dose (field magnitude)-dependent manner. Horizontal axis represents the rank order of the field strength in each region of interest (ROI) of the Power atlas. Blue curve (associated with blue labels on *left* axis) shows the estimated field strength in each of the ROIs. Red curve (associated with *right* axis) shows the excess change in FC for left hMT+ (ΔFC$_{L-R}$) for each ROI. Green curve (associated with green labels on *left* axis) shows the fraction of ROIs in the left hemisphere. For visualization purposes only, all curves were smoothed (25 nearest neighbors); line shading spans 1 SE of the mean across subjects. Graph shows that ΔFC$_{L-R}$ was larger in ROIs with larger field strengths. See main text for the supporting statistical analysis.

ΔFC$_{L-R}$; for ROIs with small field strengths (*left* on the horizontal axis), the changes were near zero. The green curve shows that most (~70%) of these ROIs were in the right hemisphere. In ROIs with field strengths above ~0.1 V/m (with the majority of ROIs from the left hemisphere) ΔFC$_{L-R}$ started to increase with field strength resulting in an overall positive association between field strength and changes in FC.

We performed the same analysis at the level of networks of the Power atlas (see MATERIALS AND METHODS). The change in FC of left and right hMT+ with the networks of the Power atlas (ΔFC^N; see MATERIALS AND METHODS) depended on the field strength in each of the target networks [$t(256) = 2.26$, $P = 0.02$], and there was an interaction with the MT hemifield [$t(256) = 2.68$, $P = 0.008$], with larger effects for left hMT+ than for right hMT+. The interaction effect ΔFC$^N_{L-R}$ also depended significantly on the field strength in the target ROIs [$t(128) = 2.28$, $P = 0.024$]. Figure 10 illustrates this relationship. Notably, it shows that the only network for which FC changed significantly (Fig. 7*B*), the dorsal attention network, also received the largest field strength.

DISCUSSION

We investigated how tACS affects BOLD signals in area hMT+ during the processing of a visual motion stimulus. Consistent with our predictions based on behavioral and electrophysiological data, we found that tACS reduced adaptation. We also observed that the application of tACS increased functional connectivity between the hMT+ and the rest of the brain, and the dorsal attention network in particular. Intracranial field estimates based on individualized finite element current-flow models showed that increases in FC depended on the field strength in both the seed and target areas, with larger fields resulting in larger FC.
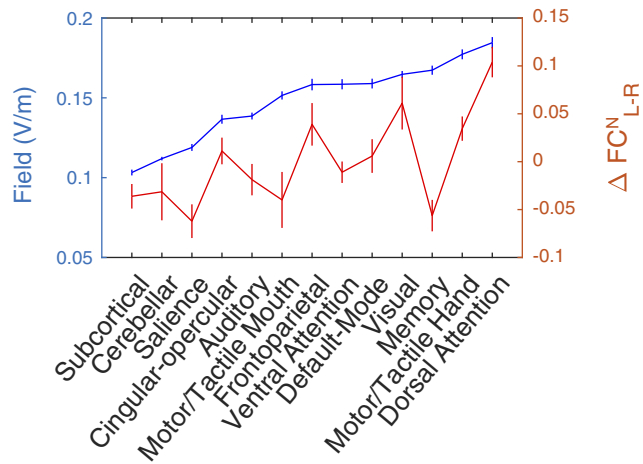
Fig. 10. Transcranial alternating current stimulation (tACS) increases network-level functional connectivity (FC^N) with human motion area (hMT+) in a dose (field magnitude)-dependent manner. Horizontal axis represents the 12 networks of the Power atlas. Blue curve (associated with *left* axis) shows the 90th percentile of the field strength across the regions of interest of the corresponding network. Networks were rank ordered with respect to this measure. Red curve (associated with *right* axis) represents the excess change in FC of the left hMT+ compared with the right hMT+ (ΔFC^N_{L-R}). Error bars span 1 SE of the mean across subjects. With a notable exception of the memory retrieval network, networks with large field magnitudes had the largest FC changes. See main text for the supporting statistical analysis.

We first address some of the potential confounding factors and limitations in the interpretation of our data and link our findings to previous studies using concurrent fMRI and tACS. We then speculate on the neural mechanisms that could be responsible for the tACS-effects we have reported and conclude with a brief discussion of the implications of our findings for the future use and interpretation of tACS-effects.

Confounding Factors

Phosphenes. Application of tACS produces phosphenes via retinal stimulation (Kar and Krekelberg 2012; Laakso and Hirata 2013; Schutter 2016; Schutter and Hortensius 2010). Phosphenes can act as a distractor and thereby reduce attention, which reduces adaptation (Rezec et al. 2004). However, this generalized effect would apply to both hemispheres. The fact that attenuation of adaptation in the left hemisphere was larger than in the right hemisphere therefore controls for this confound, and we conclude that the attenuation of adaptation is not a side effect of phosphenes or any stimulation-induced overall changes in arousal or attention.

Artifacts introduced by tACS in the scanner. Antal et al. (2014) showed that transcranially applied direct currents can produce artifacts in the EPI signal on the scalp and in the cerebrospinal fluid. Under the same conditions, however, 40-Hz tACS did not result in significant artifacts. A similar conclusion was drawn at ~10-Hz tACS by Williams et al. (2017). Taken together, these findings suggest that the BOLD signals we measured are unlikely to be affected greatly by stimulation artifacts.

tACS Mechanism

These results provide novel support for our hypothesis that tACS attenuates adaptation. First, they provide the first evidence that tACS reduces neural adaptation in the human brain

as it does in the nonhuman primate (Kar et al. 2017). Second, using BOLD imaging, we could analyze the effects of tACS during stimulation, a period we could not consider in the nonhuman primate recordings because of the electrical artifacts in the sensitive electrophysiological recording hardware (Liu et al. 2018). Because an increase in neural activity during stimulation should result in an increase in adaptation, this suggests that tACS also interferes with the cellular mechanisms of adaptation (i.e., downstream from the increase in firing rate).

The current data do not address the mechanistic details at the cellular level, but we have previously speculated that small membrane voltage fluctuations may interact with the dynamics of the Na^+- and Ca^{2+}-activated K^+ channels that underlie visual adaptation, analogous to findings in the hippocampus (Fernandez et al. 2011). Of course, this is only one potential mechanism, and finding the true cellular mechanism(s) likely requires in vitro recordings or the use of transgenic animals in which specific channels can be expressed selectively (Stroud et al. 2012).

Our finding that 10-Hz tACS increased the BOLD response to the onset of a visual stimulus appears to conflict with previous reports demonstrating a decrease in stimulus-driven BOLD response (Cabral-Calderin et al. 2016a; Vosskuhl et al. 2016). One potential explanation of this discrepancy is that our montage primarily targeted parietal cortex, whereas the Oz/Cz montage of earlier studies targeted occipital cortex. Occipital cortex is dominated by alpha oscillations, and their power correlates negatively with the BOLD signal (Scheeringa et al. 2012). This suggests that tACS entrainment of alpha could reduce the BOLD signal, but only in early visual cortex (Vosskuhl et al. 2016). Such areal specificity of tACS is intriguing and potentially powerful, because it suggests that cortical targeting could be achieved not just by choosing appropriate electrode montages but also by the selection of particular stimulation frequencies (Cabral-Calderin et al. 2016a).

Functional Connectivity

Our FC analysis found direct evidence that 10-Hz tACS increased FC (e.g., ΔGBC_{L-R} of hMT+ and ΔFC^N_{L-R} of hMT+ and the DAN), but the strongest evidence supporting the claim that tACS increases FC more generally comes from the fact that changes in FC between two areas depended on the field strength in both areas. This can, for instance, be inferred from the fact that left hMT+ (with the stronger field) increased its connectivity more than right hMT+, areas with larger fields increased their GBC more, and connectivity increases of a seed area (left hMT+) increased in proportion to the fields in the target ROI.

The finding that hMT+ mainly increased connectivity with the dorsal attention network (DAN; which includes the intraparietal sulci and frontal eye fields; Fig. 6*B*) is therefore likely primarily a result of the large fields that our montage created in the DAN (Fig. 10) (although the role of other factors cannot be excluded). Notably, the association of FC increases and field strength is far from perfect; the memory network, for instance, received almost the same field as the DAN, and yet its FC was only minimally affected by tACS. This suggests that some intrinsic properties of the memory network, its connectivity with hMT+, or idiosyncrasies of the visual task (which, for

instance, contained no memory component) played a role in the ability of tACS to modulate FC. Hence, even though our data show a reliable influence of field strength on the modulation of FC, generalizing this insight to other tasks or contexts need not be straightforward. The complex and sometimes contradictory findings in previous work support this view; the ability of tACS to modulate FC depends on brain areas, stimulation frequencies, electrode montages, and tasks (Cabral-Calderin et al. 2016b, 2016a). Nevertheless, our findings suggest that individualized head models could help to unravel these complexities.

Targeted Stimulation

Large stimulation electrodes are appealing because they result in low current densities, which limits tactile and/or painful sensations on the scalp. However, the electric field calculations (Fig. 8) show that such electrodes generate fields that spread widely in the brain. In our specific montage, the fields in the target area (left hMT+) were approximately twofold larger than those in the opposite hemisphere. In the macaque (Kar et al. 2017), we used an analogous stimulation approach but measured the fields intracranially. There, the target area received an electric field that was four times larger than that in the opposite hemisphere. Given the numerous technical differences between these studies and the species differences, this seems a reasonable level of agreement. Both studies show that some spatial targeting can be achieved even with large pad electrodes, but off-target stimulation that is 25–50% of the targeted stimulation magnitude can be expected even in the opposite hemisphere. Within the same hemisphere, spatial targeting is even more limited and off-target stimulation often occurs at equal or greater magnitude, especially in brain areas near the ventricles (Alekseichuk et al. 2019; Huang et al. 2017, 2019).

Interestingly, our electrophysiological and fMRI data provide evidence that two- to fourfold differences in field strength, even at a low (<1 V/m) overall magnitude, are sufficient to induce measurable differences in neural activity. This upside (small field differences result in measurable activity differences) also has a downside in that it limits the interpretation of tACS experiments. For instance, we cannot infer (based on these data alone) that the stimulation of hMT+ directly causes the reduction in behavioral measures of adaptation (Kar and Krekelberg 2014), because off-target stimulation (i.e., outside hMT+) is not negligible compared with on-target stimulation. Such restrictions on the interpretation of causality will apply to most, if not all, tACS experiments. In other words, even if stimulation targeted to brain area X results in a behavioral change, that does not prove that X is causally involved in the behavior.

Conclusion

Our analyses show that tACS applied during prolonged visual motion stimulation increases activity in hMT+ and yet reduces the influence of the prolonged exposure on subsequent responses. We conclude that tACS attenuates the induction of adaptation in the human brain as it does in the monkey brain (Kar et al. 2017). In addition, we found that tACS increases functional connectivity between areas that receive strong fields in a dose-dependent manner. In our particular montage this primarily resulted in increased connectivity between hMT+

and the dorsal attention network. Our data show that the changes in activity, adaptation, and functional connectivity are at least partially independent. We speculate that making an area less adapted, more active, and more strongly connected could contribute to the cognitive enhancements reported using tACS.

DISCLAIMERS

The funding sources were not involved in study design, data collection and interpretation, or the decision to submit the work for publication. The content is solely the responsibility of the authors and does not necessarily represent the official views of the funding agencies.

DISCLOSURES

No conflicts of interest, financial or otherwise, are declared by the authors.

AUTHOR CONTRIBUTIONS

K.K. and B.K. conceived and designed research; K.K. performed experiments; K.K., T.I., and B.K. analyzed data; K.K. and B.K. interpreted results of experiments; K.K. and T.I. prepared figures; B.K. drafted manuscript; K.K. and B.K. edited and revised manuscript; K.K., T.I., M.W.C., and B.K. approved final version of manuscript.

REFERENCES

Alekseichuk I, Diers K, Paulus W, Antal A. Transcranial electrical stimulation of the occipital cortex during visual perception modifies the magnitude of BOLD activity: a combined tES-fMRI approach. *Neuroimage* 140: 110–117, 2016. doi:10.1016/j.neuroimage.2015.11.034.

Alekseichuk I, Mantell K, Shirinpour S, Opitz A. Comparative modeling of transcranial magnetic and electric stimulation in mouse, monkey, and human. *Neuroimage* 194: 136–148, 2019. doi:10.1016/j.neuroimage.2019.03.044.

Ali MM, Sellers KK, Fröhlich F. Transcranial alternating current stimulation modulates large-scale cortical network activity by network resonance. *J Neurosci* 33: 11262–11275, 2013. doi:10.1523/JNEUROSCI.5867-12.2013.

Anstis S, Verstraten FA, Mather G. The motion aftereffect. *Trends Cogn Sci* 2: 111–117, 1998. doi:10.1016/S1364-6613(98)01142-5.

Antal A, Bikson M, Datta A, Lafon B, Dechent P, Parra LC, Paulus W. Imaging artifacts induced by electrical stimulation during conventional fMRI of the brain. *Neuroimage* 85: 1040–1047, 2014. doi:10.1016/j.neuroimage.2012.10.026.

Antal A, Boros K, Poreisz C, Chaieb L, Terney D, Paulus W. Comparatively weak after-effects of transcranial alternating current stimulation (tACS) on cortical excitability in humans. *Brain Stimul* 1: 97–105, 2008. doi:10.1016/j.brs.2007.10.001.

Cabral-Calderin Y, Weinrich CA, Schmidt-Samoa C, Poland E, Dechent P, Bähr M, Wilke M. Transcranial alternating current stimulation affects the BOLD signal in a frequency and task-dependent manner. *Hum Brain Mapp* 37: 94–121, 2016a. doi:10.1002/hbm.23016.

Cabral-Calderin Y, Williams KA, Opitz A, Dechent P, Wilke M. Transcranial alternating current stimulation modulates spontaneous low frequency fluctuations as measured with fMRI. *Neuroimage* 141: 88–107, 2016b. doi:10.1016/j.neuroimage.2016.07.005.

Cole MW, Ito T, Schultz D, Mill R, Chen R, Cocuzza C. Task activations produce spurious but systematic inflation of task functional connectivity

estimates. *Neuroimage* 189: 1–18, 2019. doi:10.1016/j.neuroimage.2018.12.054.

Cole MW, Pathak S, Schneider W. Identifying the brain's most globally connected regions. *Neuroimage* 49: 3132–3148, 2010. doi:10.1016/j.neuroimage.2009.11.001.

Cole MW, Yarkoni T, Repovs G, Anticevic A, Braver TS. Global connectivity of prefrontal cortex predicts cognitive control and intelligence. *J Neurosci* 32: 8988–8999, 2012. doi:10.1523/JNEUROSCI.0536-12.2012.

Cox RW. AFNI: software for analysis and visualization of functional magnetic resonance neuroimages. *Comput Biomed Res* 29: 162–173, 1996. doi:10.1006/cbmr.1996.0014.

Engel SA. Adaptation of oriented and unoriented color-selective neurons in human visual areas. *Neuron* 45: 613–623, 2005. doi:10.1016/j.neuron.2005.01.014.

Esteban O, Markiewicz CJ, Blair RW, Moodie CA, Isik AI, Erramuzpe A, Kent JD, Goncalves M, DuPre E, Snyder M, Oya H, Ghosh SS, Wright J, Durnez J, Poldrack RA, Gorgolewski KJ. fMRIPrep: a robust preprocessing pipeline for functional MRI. *Nat Methods* 16: 111–116, 2019. doi:10.1038/s41592-018-0235-4.

Fang F, Murray SO, Kersten D, He S. Orientation-tuned fMRI adaptation in human visual cortex. *J Neurophysiol* 94: 4188–4195, 2005. doi:10.1152/jn.00378.2005.

Fernandez FR, Broicher T, Truong A, White JA. Membrane voltage fluctuations reduce spike frequency adaptation and preserve output gain in CA1 pyramidal neurons in a high-conductance state. *J Neurosci* 31: 3880–3893, 2011. doi:10.1523/JNEUROSCI.5076-10.2011.

Francis JT, Gluckman BJ, Schiff SJ. Sensitivity of neurons to weak electric fields. *J Neurosci* 23: 7255–7261, 2003. doi:10.1523/JNEUROSCI.23-19-07255.2003.

Fröhlich F, McCormick DA. Endogenous electric fields may guide neocortical network activity. *Neuron* 67: 129–143, 2010. doi:10.1016/j.neuron.2010.06.005.

Helfrich RF, Knepper H, Nolte G, Strüber D, Rach S, Herrmann CS, Schneider TR, Engel AK. Selective modulation of interhemispheric functional connectivity by HD-tACS shapes perception. *PLoS Biol* 12: e1002031, 2014a. doi:10.1371/journal.pbio.1002031.

Helfrich RF, Schneider TR, Rach S, Trautmann-Lengsfeld SA, Engel AK, Herrmann CS. Entrainment of brain oscillations by transcranial alternating current stimulation. *Curr Biol* 24: 333–339, 2014b. doi:10.1016/j.cub.2013.12.041.

Herrmann CS, Rach S, Neuling T, Strüber D. Transcranial alternating current stimulation: a review of the underlying mechanisms and modulation of cognitive processes. *Front Hum Neurosci* 7: 279, 2013. doi:10.3389/fnhum.2013.00279.

Huang Y, Datta A, Bikson M, Parra LC. Realistic volumetric-approach to simulate transcranial electric stimulation–ROAST–a fully automated open-source pipeline. *J Neural Eng* 16: 056006, 2019. doi:10.1088/1741-2552/ab208d.

Huang Y, Liu AA, Lafon B, Friedman D, Dayan M, Wang X, Bikson M, Doyle WK, Devinsky O, Parra LC. Measurements and models of electric fields in the *in vivo* human brain during transcranial electric stimulation. *eLife* 6: e18834, 2017. doi:10.7554/eLife.18834.

Huk AC, Ress D, Heeger DJ. Neuronal basis of the motion aftereffect reconsidered. *Neuron* 32: 161–172, 2001. doi:10.1016/S0896-6273(01)00452-4.

Ito T, Kulkarni KR, Schultz DH, Mill RD, Chen RH, Solomyak LI, Cole MW. Cognitive task information is transferred between brain regions via resting-state network topology. *Nat Commun* 8: 1027, 2017. doi:10.1038/s41467-017-01000-w.

Kar K. Commentary: on the possible role of stimulation duration for aftereffects of transcranial alternating current stimulation. *Front Cell Neurosci* 9: 148, 2015. 10.3389/fnsys.2015.00148.

Kar K, Duijnhouwer J, Krekelberg B. Transcranial alternating current stimulation attenuates neuronal adaptation. *J Neurosci* 37: 2325–2335, 2017. doi:10.1523/JNEUROSCI.2266-16.2016.

Kar K, Krekelberg B. Transcranial electrical stimulation over visual cortex evokes phosphenes with a retinal origin. *J Neurophysiol* 108: 2173–2178, 2012. doi:10.1152/jn.00505.2012.

Kar K, Krekelberg B. Transcranial alternating current stimulation attenuates visual motion adaptation. *J Neurosci* 34: 7334–7340, 2014. doi:10.1523/JNEUROSCI.5248-13.2014.

Kar K, Krekelberg B. Testing the assumptions underlying fMRI adaptation using intracortical recordings in area MT. *Cortex* 80: 21–34, 2016. doi:10.1016/j.cortex.2015.12.011.

Kohn A. Visual adaptation: physiology, mechanisms, and functional benefits. *J Neurophysiol* 97: 3155–3164, 2007. doi:10.1152/jn.00086.2007.

Krause MR, Vieira PG, Csorba BA, Pilly PK, Pack CC. Transcranial alternating current stimulation entrains single-neuron activity in the primate brain. *Proc Natl Acad Sci USA* 116: 5747–5755, 2019. doi:10.1073/pnas.1815958116.

Krekelberg B, Boynton GM, van Wezel RJ. Adaptation: from single cells to BOLD signals. *Trends Neurosci* 29: 250–256, 2006a. doi:10.1016/j.tins.2006.02.008.

Krekelberg B, van Wezel RJ, Albright TD. Adaptation in macaque MT reduces perceived speed and improves speed discrimination. *J Neurophysiol* 95: 255–270, 2006b. doi:10.1152/jn.00750.2005.

Laakso I, Hirata A. Computational analysis shows why transcranial alternating current stimulation induces retinal phosphenes. *J Neural Eng* 10: 046009, 2013. doi:10.1088/1741-2560/10/4/046009.

Larsson J, Landy MS, Heeger DJ. Orientation-selective adaptation to first- and second-order patterns in human visual cortex. *J Neurophysiol* 95: 862–881, 2006. doi:10.1152/jn.00668.2005.

Liu A, Vöröslakos M, Kronberg G, Henin S, Krause MR, Huang Y, Opitz A, Mehta A, Pack CC, Krekelberg B, Berényi A, Parra LC, Melloni L, Devinsky O, Buzsáki G. Immediate neurophysiological effects of transcranial electrical stimulation. *Nat Commun* 9: 5092, 2018. doi:10.1038/s41467-018-07233-7.

Ozen S, Sirota A, Belluscio MA, Anastassiou CA, Stark E, Koch C, Buzsáki G. Transcranial electric stimulation entrains cortical neuronal populations in rats. *J Neurosci* 30: 11476–11485, 2010. doi:10.1523/JNEUROSCI.5252-09.2010.

Patterson CA, Duijnhouwer J, Wissig SC, Krekelberg B, Kohn A. Similar adaptation effects in primary visual cortex and area MT of the macaque monkey under matched stimulus conditions. *J Neurophysiol* 111: 1203–1213, 2014. doi:10.1152/jn.00030.2013.

Power JD, Cohen AL, Nelson SM, Wig GS, Barnes KA, Church JA, Vogel AC, Laumann TO, Miezin FM, Schlaggar BL, Petersen SE. Functional network organization of the human brain. *Neuron* 72: 665–678, 2011. doi:10.1016/j.neuron.2011.09.006.

Rezec A, Krekelberg B, Dobkins KR. Attention enhances adaptability: evidence from motion adaptation experiments. *Vision Res* 44: 3035–3044, 2004. doi:10.1016/j.visres.2004.07.020.

Rubinov M, Sporns O. Complex network measures of brain connectivity: uses and interpretations. *Neuroimage* 52: 1059–1069, 2010. doi:10.1016/j.neuroimage.2009.10.003.

Scheeringa R, Petersson KM, Kleinschmidt A, Jensen O, Bastiaansen MC. EEG α power modulation of fMRI resting-state connectivity. *Brain Connect* 2: 254–264, 2012. doi:10.1089/brain.2012.0088.

Schutter DJ. Cutaneous retinal activation and neural entrainment in transcranial alternating current stimulation: a systematic review. *Neuroimage* 140: 83–88, 2016. doi:10.1016/j.neuroimage.2015.09.067.

Schutter DJ, Hortensius R. Retinal origin of phosphenes to transcranial alternating current stimulation. *Clin Neurophysiol* 121: 1080–1084, 2010. doi:10.1016/j.clinph.2009.10.038.

Stroud AC, Ledue EE, Crowder NA. Orientation specificity of contrast adaptation in mouse primary visual cortex. *J Neurophysiol* 108: 1381–1391, 2012. doi:10.1152/jn.01148.2011.

Tootell RB, Reppas JB, Dale AM, Look RB, Sereno MI, Malach R, Brady TJ, Rosen BR. Visual motion aftereffect in human cortical area MT revealed by functional magnetic resonance imaging. *Nature* 375: 139–141, 1995. doi:10.1038/375139a0.

Vosskuhl J, Huster RJ, Herrmann CS. BOLD signal effects of transcranial alternating current stimulation (tACS) in the alpha range: a concurrent tACS-fMRI study. *Neuroimage* 140: 118–125, 2016. doi:10.1016/j.neuroimage.2015.10.003.

Williams KA, Cabral-Calderin Y, Schmidt-Samoa C, Weinrich CA, Dechent P, Wilke M. Simultaneous transcranial alternating current stimulation and functional magnetic resonance imaging. *J Vis Exp* 2017: 1–11, 2017. doi:10.3791/55866.

Zaehle T, Rach S, Herrmann CS. Transcranial alternating current stimulation enhances individual alpha activity in human EEG. *PLoS One* 5: e13766, 2010. doi:10.1371/journal.pone.0013766.